MRI Iterative Super Resolution with Wiener Filter Regularization

Marcia L. S. Aguena, Nelson D. A. Mascarenhas, Junia C. Anacleto
Departamento de Computação
UFSCar - Universidade Federal de São Carlos
São Carlos, SP - Brazil
Email: {aguena, nelson, junia}@dc.ufscar.br

Sidney S. Fels
Dept. of Electrical and Computer Engineering
The University of British Columbia
Vancouver, BC, Canada
Email: ssfels@ece.ubc.ca

***Abstract*—The swallowing process affects several aspects of one's welfare, as nutrition, hydration, respiration and hearing. Magnetic resonance imaging (MRI) has been a valuable tool to study swallowing, since it is a non-invasive procedure that can dynamically capture the shapes of the tongue and other elements involved in the process. The resolution enhancement of the MRI frames support directly diseases diagnoses, helping the visual analysis, or can be a pre-processing tool to segmentation, classification, recognition or modelling. MRI frames with better resolution, with less blurring or noise can be obtained changing the acquisition process, or using more powerful devices, but the cost of this solution is higher than applying computational Super-Resolution (SR) techniques. This paper studies a Bayesian approach to provide a Wiener filter to regularize the conjugate gradient solution, and promote an adaptation of an iterative SR method for non-rigid registration that can be generalized to other iterative SR methods.**

***Keywords*-Super-Resolution; Swallowing MRI; Wiener Filter; Conjugate Gradient; Bayesian Regularization;**

I. Introduction

Swallowing problems are fairly common and have a prevalence of $16 - 22\%$ among individuals older than 50 years. A growing interest in real-time magnetic resonance techniques for assessing swallowing has been generated by the projectional nature of the technique in conjunction with excellent soft tissue contrast. Magnetic resonance imaging (MRI) has several advantages compared with conventional X-ray techniques: No harmful side effects like radiation; variable slice orientations without changing the position of the patient; soft tissue contrast [1].

One of the first works to address a SR method to MRI was developed by Peled et al. [2]. They applied the Irani-Peleg's Iterative-Back-Projection (IBP) method [3] to original and synthetic images obtained by downsampling, blurring, shifting and adding gaussian noise to human white matter fiber tract MRI. To produce an experiment with original images, the author acquired 72 images: eight shifted images for each of nine diffusion weightings. According to the paper, the resulting SNR was about 20% better than the original one. Although it was an initial step, Scheffler [4] observed that the images were acquired with an in-plane shifted in phase encoding some subpixel displacements, using the same field-of-view (FOV) and resolution. This means that the sampled data in k-space was identical for all images, they were just sampled at different positions in image space. So, despite the Signal-Noise Ratio (SNR) increasing, the resolution enhancement could be obtained directly from the original data.

In order to create a real SR method for MRI it is necessary that the observed images present some kind of real redundance, as the similarity of two different but contiguous slices of a 3-D MRI or dynamic MRI frames. In both cases the image registration is more complex, since the difference between two frames is not uniform. Because of this, most work has concentrated on brain MRI [5], [6], [7], [8], where a simple global uniform motion registration can be applied.

To consider MRI of structures not so still as the brain, like the tongue [9] or the vocal tract [10], [11], [12] a more complex registration is needed.

Martins et al. [10] developed a method for spatio-temporal resolution enhancement of vocal tract image sequence, in a two stage approach. In the first stage the displacements and deformations, estimated by a non-rigid registration method, were used in an interpolation to generate intermediate images. In a second stage, the SR image reconstruction, applying a maximum a posteriori probability estimation based on Markov random field prior model. The iterated conditional modes (ICM) algorithm was used sequentially to update the high resolution (HR) images, making the solution computationally costly. Later in [11], Martins et al. proposed a refinement of the second stage by a novel discrete Wiener filter based on statistical interpolation of [13] (described in section II-B). Another upgrade of the same authors was made in [12], changing and comparing the separable Markovian model with the isotropic model, that empirically represents the estimated image autocorrelation.

A promising research line in MRI-SR is the sparse methods exploration. Manjon et al. [14] propose to recover some of the high frequency information in an upsampling method that uses data-adaptive patch-based reconstruction combined with a subsampling coherence constraint. In a recent work Rueda et al. [15], presents a sparse-based super-resolution method, adapted for easily including prior knowledge, which couples up high and low frequency information so that a high-resolution version of a low-resolution brain MR image is generated. The sparsity based methods of SR, as in many

others subjects in image processing as denoising, compression, impainting, restoration etc, have outperformed the pre-existing state-of-art SR methods.

Contributions: The computational SR techniques for MRI provides lower cost and higher flexibility than device changes or exposure time increase. This paper proposes an iterative MRI-SR method with a locally adapted Bayesian approach for the Conjugate Gradient (CG-SR) solution that considers the correlation between the frames. The Conjugate Gradient solution provide faster convergence rate and the Bayesian approach implements a stronger regularization than the traditional Laplacian method.

A. Technique Overview

This method applies the iterative CG-SR method to upsampling, deblurring and denoising swallowing images obtained with MRI. It provides a more reliable and flexible regularization, that allows to change it as necessary. We take this advantage to choose a Bayesian approach to formulate a Wiener filter, considering not just the pixel neighborhood but the influence of the nearest frames on it. The algorithm algebraic formulation has to be changed to accommodate the non-rigid registration, since it is appropriate to matrix formulation. To better understand this technique in section II we present the origin of the ideas applied in this work. The developed technique is described in section III. In section IV the experiments are presented and discussed. And finally, in section V, the final conclusions will be exposed.

II. Technical Background

A. The Conjugate Gradient for Super-Resolution

Irani-Peleg's IBP regularization is created during the high resolution (HR) composition by the low resolution (LR) images and is just the elimination of the outliers values in this process. The CG-SR has the same regularization as Tikhonov-Miller-SR method, but the convergence rate is higher.

In general terms, the strategy that characterizes SR can be represented by the block diagram of Figure 1.

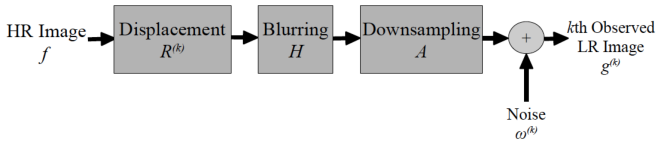

Fig. 1: Block diagram of SR image degradation process.

The degradation process responsible for the kth LR image can be described as:

$$g^{(k)} = AHR^{(k)}f + \omega^{(k)}, \qquad \forall k = 1, 2, \cdots, N \tag{1}$$

where A is the downsampling matrix, H the blurring matrix, $R^{(k)}$ the displacement from kth LR image, $g^{(k)}$ the lexicographic representation of kth observed LR image and f is the lexicographic representation of the HR image.

Choosing matrices $D^{(k)}_{AHR}$ in a way to represent the blurring, displacement and downsampling, such as $D^{(k)}_{AHR} = AHR^{(k)}$, equation (1) can be rewritten as in [16]:

$$g^{(k)} = D^{(k)}_{AHR}f + \omega^{(k)}, \qquad \forall k = 1, 2, \cdots, K \tag{2}$$

The system described by (2) is an ill-conditioned inverse problem and therefore, the iterative solution must be regularized.

There are several iterative restoration methods suitable to be adapted to SR. Aguena and Mascarenhas in [17] presented iterative SR based on Van Cittert , Tikhonov-Miller and Conjugate Gradient (CG) restoration methods. In this work, the iterative CG-SR method is described as:

$$\begin{aligned} r_i =& -\alpha C^t I^{(k)}_{rg} C f_i \\ &+ cD^{(k)t}_{AHR} I^{(k)}_{db} \sum_{k=1}^{n} (g^{(k)} - D^{(k)}_{AHR} f_i) \\ p_i =& \, r_i + \gamma_i p_{i-1}, \\ f_{i+1} =& \, f_i + \beta_i p_i. \end{aligned} \tag{3}$$

with

$$\gamma_i = \frac{\|r_i\|^2}{\|r_{i-1}\|^2} \tag{4}$$

$$\beta_i = \frac{r_i^t p_i}{\|(D^{(\circ)}_{AHR})p_i\|^2_{I_{db}} + \alpha \|Cp_i\|^2_{I_{rg}}}, \tag{5}$$

where C is a Laplacian operator to regularize the noise amplification, inherent to the deblurring process, and ^{t} is the transpose matrix notation. c is a constant to normalise the columns of A and divide the summation to obtain the mean. The $(\circ)$ is the image whose high resolution lattice is been used as reference to register all other images. So, the matrix $D^{(\circ)}_{AHR}$ represents the degradation process suffered by the $(\circ)$ image.

It is very common that iterative restoration methods produces *ringing* artifact like an echo of the high frequencies. The matrices I_{db} and I_{rg} are two diagonal matrices applied to reduce this artefact. The elements of the main diagonal of I_{db} and I_{rg} are lexicographical representation of the coefficients matrices rg and db respectively. The elements of matrices rg and db are calculated as:

$$rg_{(i,j)} = \frac{1}{1 + \mu \max\left[0, \sigma_g^2 - \sigma_\omega^2\right]} \tag{6}$$

$$db_{(i,j)} = \frac{1}{1 + (\mu \max\left[0, \sigma_g^2 - \sigma_\omega^2\right])^{-1}}, \tag{7}$$

where σ_g^2 is the local variance around $g(i,j)$ pixel and σ_ω^2 the variance of the whole image g. The operation $||\cdot||^2_Q$ is a weighted ℓ_2 norm with q_{ij} coeficients of diagonal matrix I_Q. In regions with smooth intensity transitions the local variance is approximately the noise variance, the $rg_{(i,j)}$ coefficients will not interfere with regularization but $db_{(i,j)}$ coefficients will

inhibit the deblurring process. In edge regions with larger local variance, the $rg_{(i,j)}$ coefficients will inhibit the regularization, and $db_{(i,j)}$ coefficients will allow a larger deblurring process.

B. The Bayesian Interpolation approach

Lagendijk [18] proposes a Wiener filter regularization for restoration based on *a priori* knowledge that both noise process (ω) and the original image (f) are multivariate Gaussian, with zero-mean and correlation matrices, $R_{\omega\omega} = \sigma_\omega^2 I$ and R_{ff} respectively. Thus, the direct Tikhonov-Miller model for restoration, given by:

$$f = \left[H^t H + \alpha C^t C\right]^{-1} H^t g, \tag{8}$$

can be rewritten as:

$$f = \left[H^t H + R_{\omega\omega} R_{ff}^{-1}\right]^{-1} H^t g. \tag{9}$$

Mascarenhas et al. [13] developed a Bayesian approach to multispectral image data fusion that models R_{ff}, which can be easily invertible. In this work, interpolation was applied to match images of 20x20m with 10x10m resolution, using patches as shown in Figure 2, in three multispectral bands.

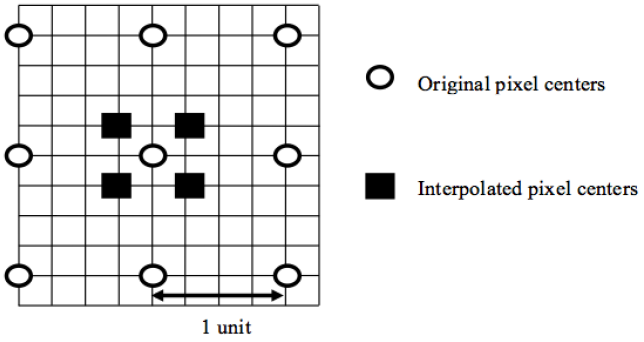

Fig. 2: Graphic representation of the Bayesian Interpolation

The vector f, is the (27×1) lexicographic ordering of the HR estimated image, and g is the (27×1) vector of the lexicographic ordering of the observed LR images. By the orhogonality principle, the interpolation process can be expressed as:

$$f = E[f] + \Sigma_{fg}\Sigma_{gg}^{-1}(g - E[g]) \tag{10}$$

where $E[.]$ is the statistical expectation, Σ_{fg} is the cross-covariance of f and g and Σ_{gg} the auto covariance of g. Since the expected values must not be changed in the interpolation process, $E[f] = E[g]$.

Assuming separability of the covariance matrices, they can be given by:

$$\Sigma_{fg} = Ch_{fg} \otimes Cv_{fg} \otimes \Sigma_S \tag{11}$$

$$\Sigma_{gg} = Ch_{gg} \otimes Cv_{gg} \otimes \Sigma_S \tag{12}$$

Under the Markovian structure the Ch matrices are given by:

$$Ch_{gg} = \begin{bmatrix} 1 & \rho_h & \rho_h^2 \\ \rho_h & 1 & \rho_h \\ \rho_h^2 & \rho_h & 1 \end{bmatrix}, \tag{13}$$

and

$$Ch_{fg} = \begin{bmatrix} \rho_h^{3/4} & \rho_h^{1/4} & \rho_h^{5/4} \\ \rho_h^{5/4} & \rho_h^{1/4} & \rho_h^{3/4} \end{bmatrix}, \tag{14}$$

where the Cv matrices have the same structure as Ch, but using ρ_v. The ρ value is the correlation coefficient of horizontal or vertical direction and they can be global or adapted to the local roughness. Zaniboni and Mascarenhas [19] implemented the local correlation coefficient to this data fusion framework. The horizontal and vertical correlation coefficients were calculated locally and with k-means algorithm they were clustered in five groups represented by its central value. Each patch of the multispectral images was mapped to one of the five groups of ρ for vertical and horizontal direction. If the neighbourhood of a pixel is smooth, the ρ value must be low, and the interpolated pixel will suffer more influence of the neighbourhood. If it is a rough area, the value of ρ is higher, and the interpolated pixel will receive less influence of the neighbourhood.

The covariance matrix between the three multispectral bands and is given by:

$$\Sigma_S = \begin{bmatrix} \sigma_{11}^2 & \sigma_{12}^2 & \sigma_{13}^2 \\ \sigma_{21}^2 & \sigma_{22}^2 & \sigma_{23}^2 \\ \sigma_{31}^2 & \sigma_{32}^2 & \sigma_{33}^2 \end{bmatrix}, \tag{15}$$

where σ_{ij}^2 is the covariance between the bands i and j, and σ_{ii}^2 is the variance of the band i.

The covariance matrix of the vector f is easily found:

$$\Sigma_f = B\Sigma_{gg}B^t = \Sigma_{fg}\Sigma_{gg}^{-1}\Sigma_{fg}^t, \tag{16}$$

where is B is given by:

$$B = \Sigma_{fg}\Sigma_{gg}^{-1}. \tag{17}$$

It should be observed that the (12×12) covariance matrix carries not only spectral information, but also information about the interpolated pixels.

Using equation (16), we can formulate R_{ff} as:

$$R_{ff} = \sigma_f^2 \Sigma_{ff}, \tag{18}$$

where σ_f^2 is the variance of f.

C. Non-Rigid Registration

To map pixels from one frame/slice to another, the corresponding anatomical and function locations must be properly found. In other words, it means to find the optimal geometric transformation that minimizes de differences between the images. The transformation model defines how this mapping, or image registration, will work. This process usually require three components:

- A transformation model to define a geometric non-rigid transformation across the images.
- A similarity metric to measure the alignment between the images.
- An optimization method to maximize the similarity metric.

The most common registration methods are based only on transformations as translations, scale or rotation. These transformations can be completely described by a fixed global set of linear weights. If no global linear model can be formulated, we have a non-linear registration. The non-linear registrations just aims to preserve the topology, avoiding tearing or collapsing regions and allowing a smooth and invertible transformation [20]. It should be noted that, registration is a critical part of the SR.

Rueckert et al. [20] developed a non-rigid image registration based on free-form deformation (FFD) and cubic B-splines interpolation. FFD is defined by a discrete three-dimensional mesh of uniformly spaced control points, each one associated with a displacement vector. A blend of this vectors define the displacement at a general location, with the nearer vector having greater influence in a region. The weight blend are determined by a weighting function and B-spline functions.

A non-rigid registration was proposed by Myronenko and Song [21], [22], and implemented in MIRT - Matlab Image Registration Toolboox (available on [23]). In this toolbox, a non-rigid registration using B-splines control points is implemented, but the goal is the variety of similarities measures as sum-of-squared differences (SSD), correlation coefficient (CC), correlation ratio (CR), and mutual information (MI). These similarities measures are based on the intensity relationship of the corresponding pixels without considering their spatial dependencies. The gradient descent optimization method is used to iteratively update the parameters of the registration.

III. MRI Iterative SR with Wiener Filter regularization

This is a novel method that adapts the iterative CG-SR method to MRI frames, replacing the registration matrix by a non-rigid registration function . A Wiener filter, based on the separability of spatial correlation structure, is also used as an adaptive regularization.

A. The algorithm

As explained by equations (1) and (2), $D_{AHR}^{(k)}$ holds the registration information. When the registration is a linear transformation as translation or rotation, it can easily be represented by a matrix, and to obtain the inverse registration transformation, the transpose matrix can be used. This property is not valid for non-rigid registration, and for this reason, the formulation of (3) has to be changed, representing the registration transformation as a function, instead of a matrix. The registration function $\boldsymbol{R}(l^{(ref)}, v)$ represents the transformation of v, an image vector, over $l^{(ref)}$, a reference lattice. Thus, from equation (3) and (9), if the LR images are zero-means, we have:

$$\begin{aligned} r_i = & -R_{\omega\omega}R_{ff}^{-1}f_i \\ & + \sum_{k=1}^{n} c\boldsymbol{R}\left(l^{(\circ)}, D_{AH}^{(k)t} I_{db}^{(k)}\left(g^{(k)} - D_{AH}^{(k)}\boldsymbol{R}\left(l^{(k)}, f_i\right)\right)\right) \\ p_i = & \, r_i + \gamma_i p_{i-1}, \\ f_{i+1} = & \, f_i + \beta_i p_i, \end{aligned} \tag{19}$$

with

$$\gamma_i = \frac{\|r_i\|^2}{\|r_{i-1}\|^2} \tag{20}$$

$$\beta_i = \frac{r_i^t p_i}{\|D_{AH}^{(\circ)} p_i\|_{I_{db}}^2 + p_i^t R_{\omega\omega} R_{ff}^{-1} p_i}. \tag{21}$$

The symbol $(\circ)$ emphasizes that a vector (or matrix) are associated with the reference lattice. But if the vectors (or matrix) have no explicitly indication of which lattice it belongs, it means that they are associated with the reference lattice too.

A detail that must be observed is that the adaptive constraint matrix I_{rg}, used in (3) and (5) is no more suitable to (19) and (21), but the adaptive constraint is preserved in regularization using an adaptive ρ. To simplify the method of Zaniboni and Mascarenhas [19], instead of finding five groups for horizontal and vertical directions, a mean between the value of both directions was used to calculate a single ρ for each patch, and these values were clustered and mapped for the interpolation. Figure 3 shows the ρ and I_{rg} mapping[1] to comparison.

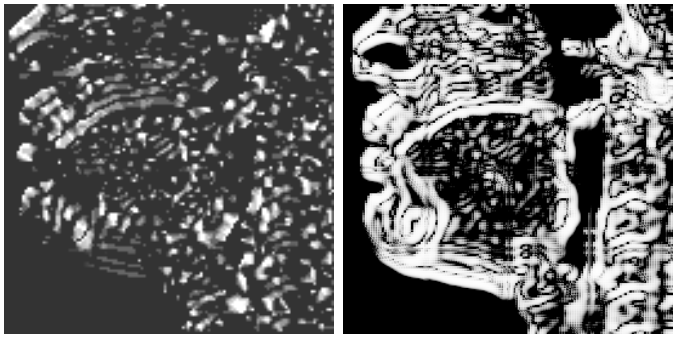

(a) ρ for noise SD=0; (b) I_{rg} for noise SD=0;

Fig. 3: Representation of ρ and I_{rg} mapping used in regularization process.

B. Initialization and tunning

The initial guess of f_0 is obtained taking the initial LR images, upsampling, registering and calculating the mean of them.

The method described in III-A has just the parameter μ to be adjusted, that in this case affects just the deblurring process, increasing the effect of the $rg_{(i,j)}$ coefficient as was explained

[1]Technically, the I_{rg} is a diagonal matrix and the Figure 3 is a map of the I_{rg} coefficients to the image.

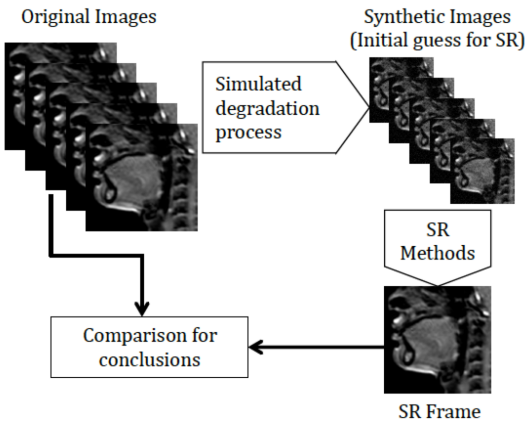

Fig. 4: Diagram of the experiment.

in II-A. Several values of μ were tested and the best results were achieved in the interval $\mu = [10^{-2}, 10^{4}]$. As we will discuss in more detail in section IV, two similarity measures were tested and the results for each measure were taken in two points: the best point of all iterations and the last one. In general, the values of μ to achieve best results increase when the degradation (blur and noise) is higher. The choice of the measure point also influences the value of μ: to the obtain the highest similarity reached in the lasts iterations, the value of μ tends to decrease. Table I shows, the values of μ that maximize the target value.

Table I: Values of μ

Blur/Noise	best SSIM	best ISNR	final SSIM	final INSR
R=2/SD=0	10^2	10^2	10^0	10^{-2}
R=2/SD=8	10^2	10^2	10^1	10^2
R=2/SD=16	10^4	10^3	10^1	10^1
R=4/SD=0	10^3	10^2	10^3	10^0
R=4/SD=8	10^3	10^3	-	-
R=4/SD=16	10^4	10^4	-	10^1

The registration procedure provided by MIRT was tested empirically and have the following parameters chosen:

- The sum of square differences (SSD) was selected as similarity measure;
- The chosen mesh windows size was 5 .The smaller the window the more complex deformations are possible, but also more regularization is required;
- 3 Hierarquical Levels were used;

IV. Experiments

The initial data for the experiments is a set of five synthetic images of 128x128 pixels, obtained from a degradation process of downsampling, blurring and additive noise, applied to a set of five 256x256 original images. Figure 5 shows the set of original frames (the central one is the reference frame witch lattice is used for registration ($\circ$)). Figure 6 (a), (f), (k) and (p) show the synthetic degraded central frame from the set that is used as initial guess to perform the experiment. The diagram of Figure 4 outlines the experiment.

The tested degradations were a combination of:

- Uniform out-of-focus blurring, with a kernel of 2 and 4 pixels of radius;
- Additive zero-mean Gaussian noise, with standard deviation (SD) of 0, 8 and 16;
- Downsampling by a factor of 2.

To compare the results of the Wiener filter (WReg) a typical Laplacian (LReg) regularization was tested with the same conditions (CG-SR method, and non-rigid registration provided by MIRT).

The quality of the process was measured by the Structural Similarity Index (SSIM) and Improvement in Signal-Noise-Ratio (ISNR). In both measures, the maximum value reached and the final value are compared.

A. Performance

The implementation was made with Matlab. The performances of the Wiener filter regularization always reach the best values, and when the degradation increases, the method tends to have a faster convergence than the Laplacian regularization. As the size of the blur grows, the process become slower, because it increases the size of the involved matrices. The same does not happen with the noise: the amount of noise does not interfere in performance.

B. Quality

The method with Wiener regularization reaches better results in most cases, but it seems to work better when the blur is small (R=2), as we can see in Figure 7 and 6. We can observe the difference between the numerical results of the methods looking at Table II and III.

Another improvement that is clearly observed but is better quantified visually is the reduction of a kind of noise, very common in MRI frames, that is not punctual but happens in spots. Figure 8 shows two frames acquired in different moments of a still person and the difference between them, to characterize this noise. Visually, the SR process reduced this noise mainly because the mean used to regroup the LR images, but we can see better results in Wiener filter regularization.

C. Limitation

A strong limitation inherent to the algebraic formulation of this method is the size of the involved matrices. To implement these methods with a reasonable amount of memory (the tests were executed in a computer with 16 GB of memory), the images were cut in 16 blocks during the debluring/regularization tasks, and put together again to register the whole image. This is time consuming, but is a safe solution.

Another point to be stressed is that the model traditional SR (equation 1) may not be the best way to express MRI image process, but the deblurring that was applied (based uniform out-of-focus blurring) can enhance the egdes of blurred images in general way, and the same can be said for the denoising process.

Fig. 5: The five original frames: the central one is the reference frame $(\circ)$.

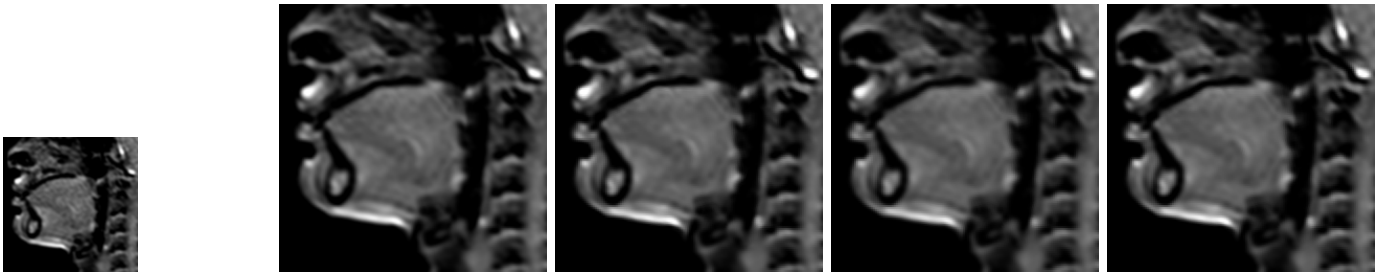

(a) blur=2, noise SD=0; (b) Best SSIM for LReg.; (c) Best SSIM for WReg.; (d) Best ISNR for LReg.; (e) Best SSIM for WReg.;

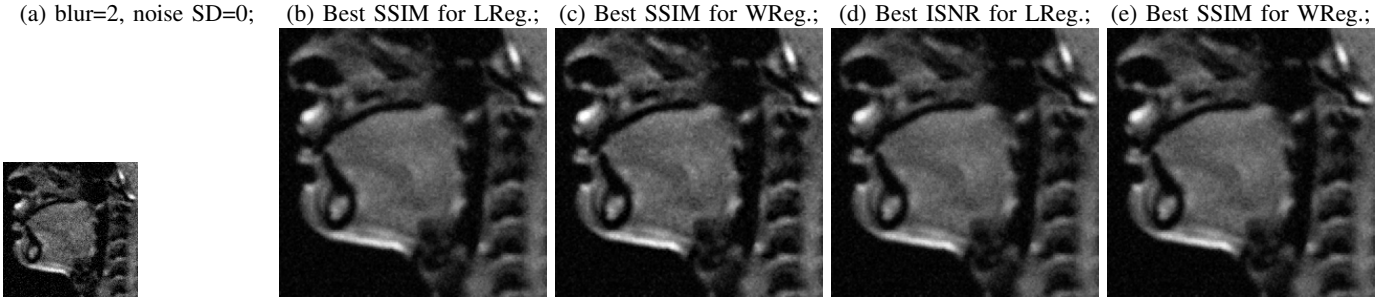

(f) blur=2, noise SD=16; (g) Best SSIM for LReg.; (h) Best SSIM for WReg.; (i) Best ISNR for LReg.; (j) Best SSIM for WReg.;

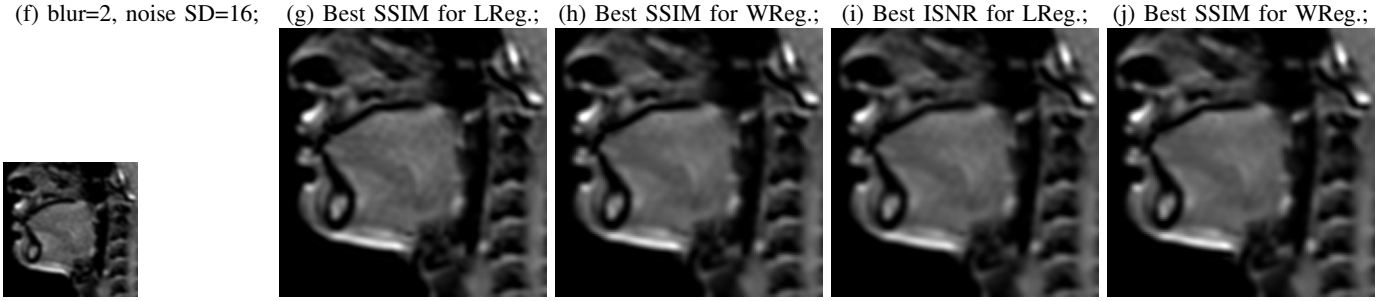

(k) blur=4, noise SD=0; (l) Best SSIM for LReg.; (m) Best SSIM for WReg.; (n) Best ISNR for LReg.; (o) Best SSIM for WReg.;

(p) blur=4, noise SD=16; (q) Best SSIM for LReg.; (r) Best SSIM for WReg.; (s) Best ISNR for LReg.; (t) Best SSIM for WReg.;

Fig. 6: Best experiments results: The first column is the initial synthetic image; the following columns are respectively the results of: the best SSIM for Laplacian regularization, the best SSIM for Wiener Filter regularization, the best ISNR for Laplacian regularization, the best ISNR for Wiener Filter regularization

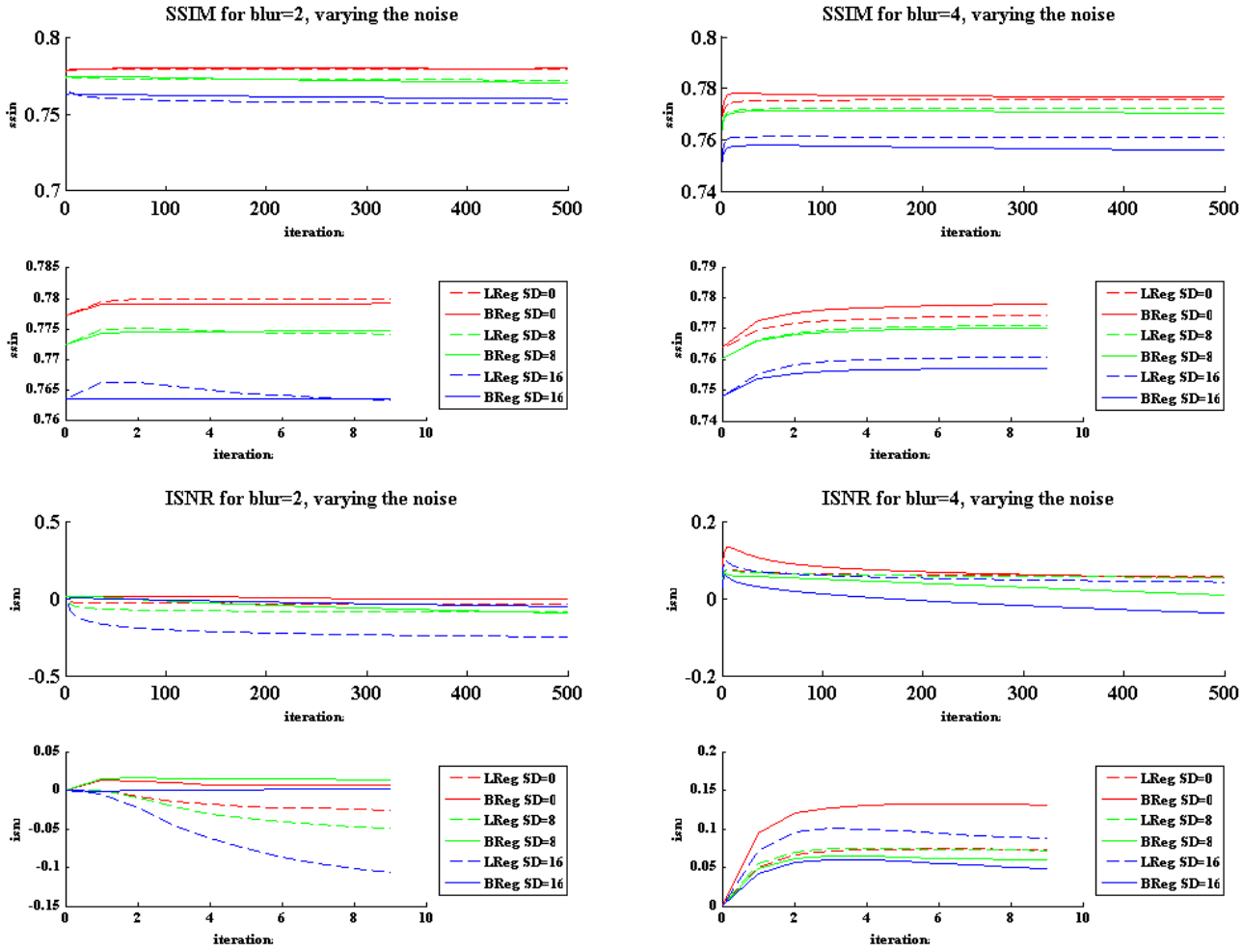

Fig. 7: Graphics comparing the behavior of the two methods for different blur and noise. The first graphic shows the total process of 500 iterations, and the second one show the details of the first 10 iterations.

Table II: Best SSIM and ISNR for Laplacian Regularization (LReg)

	best SSIM		best ISNR		final SSIM		final INSR	
Blur/Noise	**value**	**iteration**	**value**	**iteration**	**value**	**iteration**	**value**	**iteration**
R=2/SD=0	0.7800	6	0.0001	2	0.7798	500	-0.0333	500
R=2/SD=8	0.7751	3	0.0005	2	0.7727	500	-0.0897	500
R=2/SD=16	0.7663	2	0.0000	1	0.7573	500	-0.2491	500
R=4/SD=0	0.7755	50	0.0738	8	0.7755	500	0.0575	500
R=4/SD=8	0.7723	50	0.0750	5	0.7723	500	0.0547	500
R=4/SD=16	0.7612	65	0.1003	4	0.7608	500	0.0424	500

Table III: Best SSIM and ISNR for Wiener Filter Regularization (WReg)

	best SSIM		best ISNR		final SSIM		final INSR	
Blur/Noise	**value**	**iteration**	**value**	**iteration**	**value**	**iteration**	**value**	**iteration**
R=2/SD=0	0.7827	10	0.0227	6	0.7802	500	-0.0034	500
R=2/SD=8	0.7790	4	0.0401	3	0.7708	500	-0.0381	500
R=2/SD=16	0.7711	3	0.0441	2	0.7603	500	-0.0525	500
R=4/SD=0	0.7782	18	0.1346	6	0.7766	500	0.1221	500
R=4/SD=8	0.7771	11	0.1658	5	0.7701	500	0.0083	500
R=4/SD=16	0.7660	6	0.1965	3	0.7558	500	-0.0234	500

V. Conclusion

This paper proposed an iterative MRI-SR, based on Conjugate Gradient solution method, with a Bayesian approach

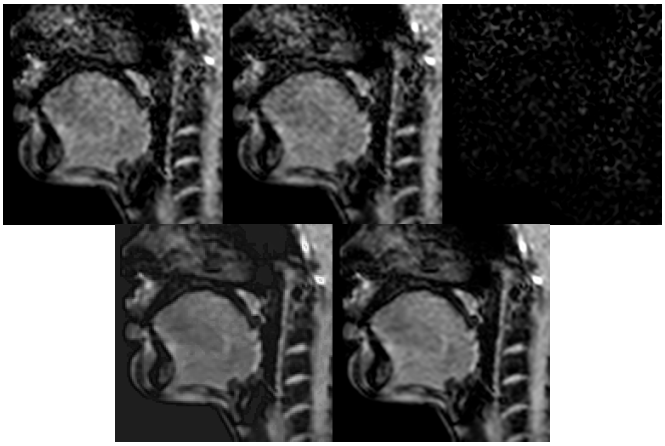

Fig. 8: Characterization of a particular kind of noise of MRI images. The first line shows two images and the difference between them. The second line shows the Wiener and Laplacian regularization results.

to provide a regularization, locally adapted to the correlation between the frames of swallowing dynamic MRI. The iterative CG-SR method had to be adapted, replacing the algebraic formulation by a function in order to perform a non-rigid registration. The Wiener filter regularization reaches better results than the Laplacian, with just a few interations, although the Wiener filter is less stable after several iterations.

Two measures of fidelity were used, the SSIM and the ISNR. The results show that the Wiener filter works better in experiments with less blur, and in this condition it was very effective to denoise the image. These characteristics are compatible with the kind of images generated by the swallowing MRI.

An undesirable characteristic of the MRI frames is a kind of deforming noise shown in Figure 8. Our method visually decreased this effects. This happens due to the nature of this SR method, that uses means to regroup the LR frames in one frame, but visually speaking the Wiener filter method also produce smoothers images.

Finally, the framework created by this method can be easily generalized to be adapted to other kinds of regularization and registration.

ACKNOWLEDGMENT

The authors would like to thank CAPES for the scholarship, and the DFAIT-CAPES program that funded the exchange program of Marcia L. S. Aguena at the University of British Columbia.

REFERENCES

[1] J. Barkhausen, M. Goyen, F. von Winterfeld, T. Lauenstein, D. Arweiler-Harbeck, and J. F. Debatin, "Visualization of swallowing using real-time true FISP MR fluoroscopy," *European radiology*, vol. 12, no. 1, pp. 129–133, 2002.

[2] S. Peled and Y. Yeshurun, "Superresolution in MRI: application to human white matter fiber tract visualization by diffusion tensor imaging," *Magnetic resonance in medicine*, vol. 45, no. 1, pp. 29–35, 2001.

[3] M. Irani and S. Peleg, "Super resolution from image sequences," in *Pattern Recognition, 1990. Proceedings., 10th International Conference on*, vol. 2. IEEE, 1990, pp. 115–120.

[4] K. Scheffler, "Superresolution in MRI?" *Magnetic resonance in medicine*, vol. 48, no. 2, pp. 408–408, 2002.

[5] A. Gholipour, J. A. Estroff, and S. K. Warfield, "Robust super-resolution volume reconstruction from slice acquisitions: application to fetal brain MRI," *Medical Imaging, IEEE Transactions on*, vol. 29, no. 10, pp. 1739–1758, 2010.

[6] X. Zhang, E. Y. Lam, E. X. Wu, and K. K. Wong, "Application of tikhonov regularization to super-resolution reconstruction of brain MRI images," in *Medical Imaging and Informatics*. Springer, 2008, pp. 51–56.

[7] R. R. Peeters, P. Kornprobst, M. Nikolova, S. Sunaert, T. Vieville, G. Malandain, R. Deriche, O. Faugeras, M. Ng, and P. Van Hecke, "The use of super-resolution techniques to reduce slice thickness in functional MRI," *International Journal of Imaging Systems and Technology*, vol. 14, no. 3, pp. 131–138, 2004.

[8] Y. Bai, X. Han, and J. L. Prince, "Super-resolution reconstruction of MR brain images," in *Proc. of 38th Annual Conference on Information Sciences and Systems (CISS04)*, 2004, pp. 1358–1363.

[9] J. Woo, Y. Bai, S. Roy, E. Z. Murano, M. Stone, and J. L. Prince, "Super-resolution reconstruction for tongue MR images," in *SPIE Medical Imaging*, vol. 8314, 2012, pp. 83 140C–83 140C–8.

[10] A. L. Martins, N. D. Mascarenhas, and C. A. Suazo, "Spatio-temporal resolution enhancement of vocal tract MRI sequences based on image registration," *Integrated Computer-Aided Engineering*, vol. 18, no. 2, pp. 143–155, 2011.

[11] A. L. Martins and N. Mascarenhas, "Spatio-temporal resolution enhancement of vocal tract MRI sequences based on the wiener filter," in *Graphics, Patterns and Images (Sibgrapi), 2011 24th SIBGRAPI Conference on*. IEEE, 2011, pp. 242–249.

[12] ——, "Wiener based spatial resolution enhancement of MRI sequences of the vocal tract: A comparison between two correlation models," in *Image Processing (ICIP), 2012 19th IEEE International Conference on*. IEEE, 2012, pp. 869–872.

[13] N. D. A. Mascarenhas, G. J. F. Banon, and A. L. B. Candeias, "Image data fusion under a bayesian approach," in *IGARSS'92*, 1992, pp. 675–677.

[14] J. V. Manjón, P. Coupé, A. Buades, V. Fonov, D. Louis Collins, and M. Robles, "Non-local MRI upsampling," *Medical image analysis*, vol. 14, no. 6, pp. 784–792, 2010.

[15] A. Rueda, N. Malpica, and E. Romero, "Single-image super-resolution of brain MR images using overcomplete dictionaries," *Medical image analysis*, pp. 113–132, 2012.

[16] A. K. Katsaggelos, R. Molina, and J. Mateos, "Super resolution of images and video," *Synthesis Lectures on Image, Video, and Multimedia Processing*, vol. 1, no. 1, pp. 1–134, 2007.

[17] M. L. Aguena and N. D. Mascarenhas, "Generalization of iterative restoration techniques for super-resolution," in *Graphics, Patterns and Images (Sibgrapi), 2011 24th SIBGRAPI Conference on*. IEEE, 2011, pp. 258–265.

[18] R. L. Lagendijk and J. Biemond, *Iterative Identification and Restoration of Images (The Springer International Series in Engineering and Computer Science)*. Springer, 1990.

[19] G. T. Zaniboni, N. Mascarenhas, T. Krug, B. F. T. Rudorff, and U. M. d. Freitas, "Fusão bayesiana de imagens utilizando coeficientes de correlação localmente adaptáveis," *Anais do IX SBSR (CDRom:\ sbsr\ 8_135o. pdf), Santos, SP (in Portuguese)*, 1998.

[20] D. Rueckert and P. Aljabar, "Nonrigid registration of medical images: Theory, methods, and applications [applications corner]," *Signal Processing Magazine, IEEE*, vol. 27, no. 4, pp. 113–119, 2010.

[21] A. Myronenko and X. Song, "Image registration by minimization of residual complexity," in *Computer Vision and Pattern Recognition, 2009. CVPR 2009. IEEE Conference on*. IEEE, 2009, pp. 49–56.

[22] ——, "Intensity-based image registration by minimizing residual complexity," *Medical Imaging, IEEE Transactions on*, vol. 29, no. 11, pp. 1882–1891, 2010.

[23] A. Myronenko. (2010) MIRT - medical image registration toolbox. Online; accessed 25-April-2013. [Online]. Available: https://sites.google.com/site/myronenko/research/mirt